

# A study of the $\pi^0\pi^0$ system produced in charge exchange and central collisions

Andrei A. Kondashov<sup>a</sup>

<sup>a</sup>IHEP, Protvino, Moscow region, 142 284 RUSSIA

On behalf of the GAMS and WA102 Collaborations

A study of the  $\pi^0\pi^0$  system produced in charge exchange  $\pi^-p$  collisions at 38 and 100 GeV/c and in central  $pp$  interactions at 450 GeV/c has been carried out. The  $S$  wave has rather a complicated structure in both processes indicating the existence of several scalar resonances. The  $f_0(980)$  and  $f_0(1500)$  appear as dips at 1 and 1.5 GeV in the  $S$  wave for charge exchange reaction, and as shoulders at these masses in the  $S$  wave for central production. The production of the  $f_0(980)$ ,  $f_0(1300)$  and  $f_0(1500)$  in the reaction  $pp \rightarrow p_f \pi^0 \pi^0 p_s$  as a function of the  $dP_T$  kinematical filter shows the behaviour differed from what has been observed for the undisputed  $q\bar{q}$  mesons. An extra  $f_0(2000)$  state is seen in the  $S$  wave for charge exchange reaction as a dip at 2 GeV. Resonances with higher spins,  $f_2(1270)$ ,  $f_4(2050)$  and  $f_6(2510)$ , have also been studied. All the three mesons are produced in the reaction  $\pi^-p \rightarrow \pi^0 \pi^0 n$  mainly via an one-pion exchange for small  $-t$ , whereas a natural-parity exchange dominates for large  $-t$ . The behaviour of the centrally produced  $f_2(1270)$  as a function of the  $dP_T$  is consistent with what has been observed for other  $q\bar{q}$  states.

## 1. INTRODUCTION

One of the most intriguing problems of the modern meson spectroscopy is the search for the gluon bound states (glueballs). A mass of the lightest scalar glueball should lie in the region 1500 – 1750 MeV as expected from the lattice QCD calculations [1, 2]. Scalar glueball candidates have been observed in several experiments. An analysis of the GAMS data on the  $IJ^{PC} = 00^{++}$  states together with the data of other experiments [3] revealed the existence of five scalar resonances in the mass range up to 1.9 GeV. One of these states is extra for  $q\bar{q}$  systematics, being a good candidate for the lightest scalar glueball.

Nevertheless, despite on considerable experimental and theoretical efforts the understanding of the scalar meson sector is rather controversial now. To identify unambiguously the scalar glueball, the structures of the scalar  $q\bar{q}$ -nonets need to be clarified, because glueball state should be superfluous for  $q\bar{q}$ -systematics. The picture may be complicated if glueball is located in the vicinity of  $q\bar{q}$ -mesons with identical quantum numbers that raises their mixing and leads to the dispersing of the glueball component over several mesons.

The  $\pi^0\pi^0$  system looks very attractive for experimental investigation and for study of the scalar resonances, in particular. Only even  $J^{PC}$  waves are present in this system, which simplifies greatly

analysis and eliminates contributions from the odd waves as compared to the  $\pi^+\pi^-$  system. Study of the  $\pi^0\pi^0$   $S$  wave in different processes should extend our knowledge about the scalar mesons and help to identify the states with enhanced gluonic component.

In the present report overview of results on the  $\pi^0\pi^0$  system produced in charge exchange reaction

$$\begin{aligned} \pi^- p &\rightarrow M^0 n \\ &\quad \downarrow \\ &\quad \pi^0 \pi^0 \rightarrow 4\gamma \end{aligned} \quad (1)$$

obtained by the GAMS Collaboration at 38 and 100 GeV/c is given and new GAMS and WA102 results on the  $\pi^0\pi^0$  system produced in the reaction

$$\begin{aligned} pp &\rightarrow p_f M^0 p_s \\ &\quad \downarrow \\ &\quad \pi^0 \pi^0 \rightarrow 4\gamma \end{aligned} \quad (2)$$

at 450 GeV/c are presented. The subscripts  $f$  and  $s$  in (2) indicate the fastest and slowest particles in the laboratory frame, respectively.

## 2. DATA SELECTION

The reaction (1) data have been obtained in two experiments carried out with the GAMS-2000 multiphoton spectrometer in 38 GeV/c  $\pi^-$  beam extracted from the 70 GeV IHEP proton accelerator (experiment SERP-E-140 at IHEP, Protvino) and

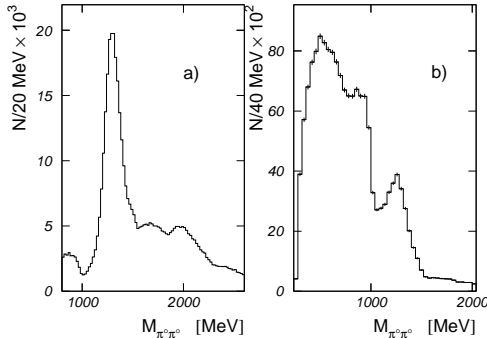


Figure 1: Invariant mass spectra of the  $\pi^0\pi^0$  system produced in reaction (1) at 100 GeV/c,  $-t < 0.2$  (GeV/c) $^2$  (a), and in reaction (2), WA102 data (b).

with the GAMS-4000 spectrometer in 100 GeV/c  $\pi^-$  beam of SPS (experiment NA12 at CERN). The general layout of the experiments, details of the GAMS-2000 and GAMS-4000 constructions and calibrations as well as event selection procedures have been given in previous publications [4, 5].

After kinematical analysis (3C fit, masses of recoil neutron and two mesons being fixed) a total of  $1.5 \times 10^6$  and  $6.5 \times 10^5$   $\pi^0\pi^0$  events are selected at 38 and 100 GeV/c, respectively. Mass spectrum of the  $\pi^0\pi^0$  events for 4-momentum transfer squared  $-t < 0.2$  (GeV/c) $^2$  is shown in fig. 1a. It is dominated by the  $f_2(1270)$ . A narrow dip corresponding to the  $f_0(980)$  is clearly seen at 1 GeV. A peak at 2 GeV is identified with the  $f_4(2050)$ . A bump around 1.7 GeV is due to the  $S$  wave contribution (see sect. 4). For  $-t > 0.2$  (GeV/c) $^2$ , the  $f_2(1270)$  peak is also clearly seen, whereas a shoulder appears on the place of the dip at 1 GeV.

The reaction (2) data come from the NA12/2 and WA102 experiments performed in 450 GeV/c proton beam of SPS at CERN. The NA12/2 experiment has been carried out with the GAMS-4000 spectrometer. The WA102 experiment has been performed using CERN Omega Spectrometer [6] and GAMS-4000.

Separation of the  $\pi^0\pi^0$  events is carried out on the basis of kinematical analysis (6C fit, four-momentum conservation being used and masses of two mesons being fixed). Events containing a fast  $\Delta^+(1232)$  are removed by imposing a cut  $M(p_f\pi^0) > 1.5$  GeV, which leave 55 000 centrally

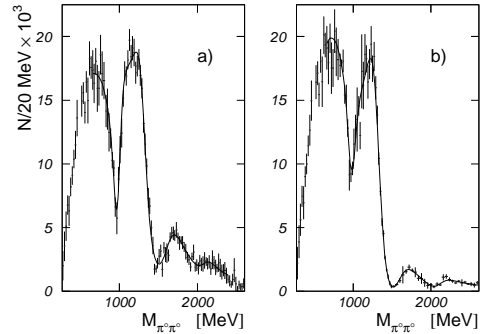


Figure 2: The  $|S|^2$  for the  $\pi^0\pi^0$  system produced in reaction (1) at 38 (a) and 100 GeV/c (b),  $-t < 0.2$  (GeV/c) $^2$ . The curves show fit with the sums of four relativistic Breit-Wigner functions and backgrounds.

produced  $\pi^0\pi^0$  events for NA12/2 and 166 000  $\pi^0\pi^0$  events for WA102.

Mass spectrum of the centrally produced  $\pi^0\pi^0$  system is shown in fig. 1b. A peak at 1.25 GeV corresponding to the  $f_2(1270)$  and a shoulder at 1 GeV which appears due to the interference of the  $f_0(980)$  with the  $S$  wave background are clearly seen.

### 3. PARTIAL WAVE ANALYSIS

For reaction (1), the coordinate system axes are defined in the Gottfried-Jackson frame. For reaction (2), the  $z$ -axis is chosen to be along the direction of the exchanged particle momentum in “slow” vertex in the  $\pi^0\pi^0$  centre of mass system, the  $y$ -axis is defined to be along cross product of the exchanged particle momenta in the  $pp$  centre of mass system.

The amplitudes used for PWA are defined in the reflectivity basis [7]. Only amplitudes with spin  $z$ -projections  $|m| = 0$  and 1 are taken into account since amplitudes with  $|m| > 1$  are equal to zero within the error bars as follows from analysis of the angular distributions. The amplitudes with spin  $l = 0, 2$  and 4 ( $S$ ,  $D$  and  $G$  waves, respectively) are used for the reaction (1) PWA at 38 GeV/c, the amplitudes with  $l = 6$  ( $J$  waves) are added at 100 GeV/c. Only  $S$  and  $D$  waves are considered for reaction (2). Contribution of the higher waves is negligibly small in the mass ranges under study for each reaction.

#### 4. REACTION $\pi^- p \rightarrow \pi^0 \pi^0 n$

The  $S$  wave amplitude module squared for the physical solution found for  $-t < 0.2$  (GeV/c)<sup>2</sup> [5, 8] is shown in fig. 2. The  $S$  wave has rather a complicated structure. It demonstrates a series of bumps separated with dips at 1, 1.5 and 2 GeV. The two first dips point to the existence of the  $f_0(980)$  and  $f_0(1500)$  resonances. Rapid variation of the relative phase of the  $S$  and  $D_0$  waves at 1 and 1.5 GeV confirms the presence of these resonances. The dip at 2 GeV is clearly seen at 100 GeV/c, it is less prominent at 38 GeV/c due to insufficient detection efficiency at high mass. This dip indicates the presence of a new scalar resonance around 2 GeV. Such conclusion is confirmed by the fast variation of the  $S$  wave phase in this mass region [5].

A simultaneous  $K$ -matrix analysis of the GAMS data on the  $S$  wave in the  $\pi^0 \pi^0$ ,  $\eta \eta$  and  $\eta \eta'$  systems produced in charge exchange reactions at 38 GeV/c in the mass range below 1.9 GeV together with the Crystal Barrel, CERN-Münich and BNL data [3] points to the existence of four comparatively narrow scalar resonances  $f_0(980)$ ,  $f_0(1300)$ ,  $f_0(1500)$  and  $f_0(1780)$  and one broad scalar state  $f_0(1530)$  with a width of about 1 GeV. The poles of the partial amplitude corresponding to physical states are determined by the mixture of input (“bare”) states related to the  $K$ -matrix poles via their transition into real mesons. The analysis [3] shows that one bare state in the mass region 1.2 – 1.6 GeV is superfluous for the  $q\bar{q}$ -classification, being a good candidate for the lightest scalar glueball. This superfluous bare state is dispersed over neighbouring physical states: the narrow  $f_0(1300)$  and  $f_0(1500)$  resonances and the broad  $f_0(1530)$ .

For  $-t > 0.3$  (GeV/c)<sup>2</sup>, a narrow peak is seen in the  $S$  wave on the place of the dip at 1 GeV observed at low momentum transfer (fig. 3) [8, 9]. A mass  $997 \pm 5$  MeV and a width  $48 \pm 10$  MeV of the peak are in good agreement with the tabulated  $f_0(980)$  parameters [10].

A simultaneous analysis of the GAMS data on the  $\pi^0 \pi^0$   $S$  wave around 1 GeV together with the Crystal Barrel and CERN-Münich data [11] shows that the  $f_0(980)$  is strongly related to the  $\pi\pi$  channel and much weaker to the  $K\bar{K}$  channel (ratio of  $f_0(980)$  coupling constants squared to the  $\pi\pi$  and  $K\bar{K}$  channels is equal to 6). This fact, together

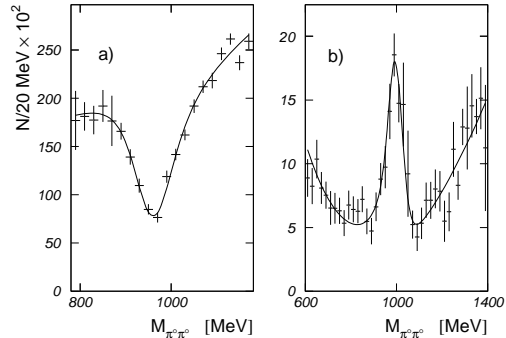


Figure 3: The  $|S|^2$  for the  $\pi^0 \pi^0$  system produced in reaction (1) at 38 GeV/c,  $-t < 0.2$  (GeV/c)<sup>2</sup> (a) and  $-t > 0.3$  (GeV/c)<sup>2</sup> (b). The curves show fit with the sums of relativistic Breit-Wigner functions and polynomial backgrounds.

with the evidence for the hard component in the  $f_0(980)$  at high  $-t$ , makes unconvincing the interpretation of this scalar meson as a  $K\bar{K}$  molecule.

Mesons with higher spins,  $f_2(1270)$ ,  $f_4(2050)$  and  $f_6(2510)$ , are seen as clear peaks in the  $D$ ,  $G$  and  $J_0$  waves, respectively (fig. 4). For  $-t < 0.2$  (GeV/c)<sup>2</sup>, all the three mesons are produced via an one pion exchange with a small absorption. Ratios of the  $f_2(1270)$  amount in the  $D$  waves with  $|m| = 0$  and 1 are equal to 7% at 38 GeV/c and 3% at 100 GeV/c [5, 9]. The ratios of the  $f_4(2050)$  amount in the  $G_0$  and  $G_{\pm}$  waves are the same as those for the  $f_2(1270)$  in the  $D$  waves. As for the  $f_6(2510)$ , the upper limit is set for its production in the  $J_{\pm}$  waves as compared to the  $J_0$  wave ( $< 0.1$ , 95% C.L.) [5].

With momentum transfer increase, an unnatural-parity exchange is died away. For  $-t > 0.3$  (GeV/c)<sup>2</sup>, the  $f_2(1270)$  and  $f_4(2050)$  are produced predominantly via a natural-parity exchange ( $D_+$  and  $G_+$  waves). This shows a similarity of the production mechanisms of the  $f_2(1270)$  and  $f_4(2050)$ .

#### 5. A KINEMATICAL $dP_T$ FILTER

Production of the states with valence gluons may be enhanced using glue-rich production mechanisms. One such mechanism is Double Pomeron Exchange (DPE) where the pomeron is thought to be a multi-gluonic object. With increasing en-

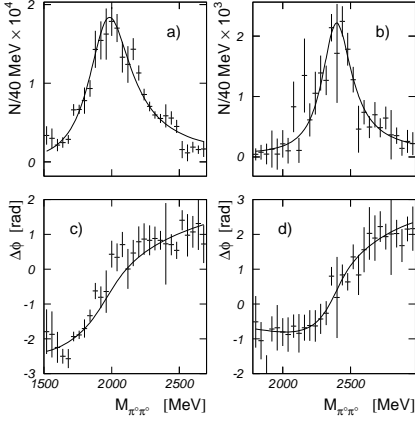


Figure 4: The  $|G_0|^2$  (a) and  $|J_0|^2$  (b) and phases of the  $G_0$  (c) and  $J_0$  (d) waves relative to the  $D_0$  wave phase for the  $\pi^0\pi^0$  system produced in reaction (1) at 100 GeV/c,  $-t < 0.2$  (GeV/c) $^2$ . The curves show fit with the sums of relativistic Breit-Wigner functions and polynomial backgrounds.

ergy, Double Pomeron Exchange (DPE) becomes relatively more important in central production with respect to other exchange processes (Reggeon-Pomeron and Reggeon-Reggeon exchange) [12].

Recently it has been proposed [13, 14] to analyse the centrally produced resonances in terms of the difference in transverse momenta of the exchanged particles which is defined as follows

$$dP_T = \sqrt{(P_{y1} - P_{y2})^2 + (P_{z1} - P_{z2})^2} \quad (3)$$

where  $P_{yi}$ ,  $P_{zi}$  are the  $y$  and  $z$  components of the momentum of the  $i$ -th exchanged particle in the  $pp$  centre of mass system. It has been observed that all the undisputed  $q\bar{q}$  states (i.e.  $\rho^0(770)$ ,  $\eta'$ ,  $f_1(1285)$ ,  $f_2(1270)$ ,  $f_2'(1525)$  etc.) are suppressed at small  $dP_T$ , whereas the glueball candidates  $f_0(1500)$ ,  $f_J(1710)$  and  $f_2(1900)$  survive.

Figure 5 shows the ratios of the event numbers for different resonances for small and large  $dP_T$  found from the fit to the efficiency corrected mass spectra. It is clearly seen that all the undisputed  $q\bar{q}$  states which can be produced in DPE have very small values for this ratio ( $\leq 0.1$ ). Some states which can not be produced by DPE (namely those with negative  $G$  parity or  $I = 1$ ) have slightly higher values ( $\approx 0.25$ ). However, all of these states are suppressed relative to the non- $q\bar{q}$  candidates

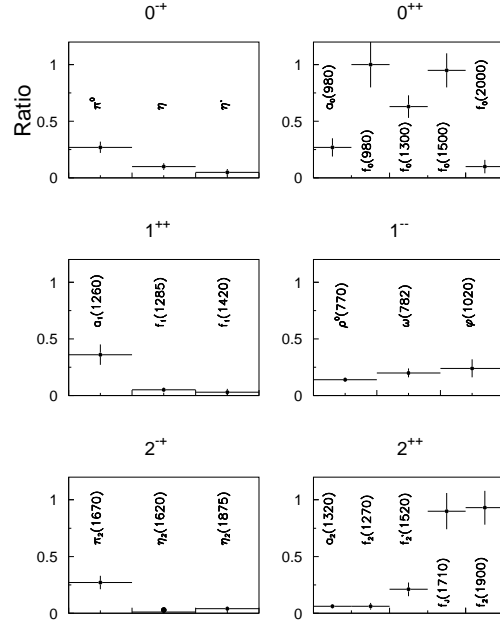


Figure 5: The ratios of the amounts of resonances with  $dP_T < 0.2$  GeV/c to the amounts with  $dP_T > 0.5$  GeV/c.

$f_0(980)$ ,  $f_0(1300)$ ,  $f_0(1500)$ ,  $f_J(1710)$  and  $f_2(1900)$  which have values for this ratio of about 1.

## 6. REACTION $pp \rightarrow p_f \pi^0 \pi^0 p_s$

A PWA of the reaction  $pp \rightarrow p_f \pi^0 \pi^0 p_s$  has been carried out in the mass range from the threshold up to 1.8 GeV. The  $S$  wave amplitude for one of the two PWA solutions is much smaller than amplitudes of the  $D$  waves in the whole mass range. This solution is rejected as unphysical one.

The  $S$  wave for the physical solution is characterized by a broad bump below 1 GeV and two shoulder, at 1 and 1.4 GeV (fig. 6). The first shoulder is attributed to the  $f_0(980)$ , the second one may be explained by the interference of the  $f_0(1300)$  and  $f_0(1500)$  resonances (see sect. 6). Peaks corresponding to the  $f_2(1270)$  are seen in the  $D_0$  and  $D_-$  waves, such peak is absent in the  $D_+$  wave. Ratio of the  $D_-$  and  $D_0$  wave intensities is about 20% at the  $f_2(1270)$  mass.

In order to apply the kinematical  $dP_T$  filter, PWA have been performed in intervals  $dP_T < 0.35$  GeV/c,  $0.35 < dP_T < 0.6$  GeV/c and  $dP_T > 0.6$  GeV/c. The shoulders at 1 and 1.4 GeV in the

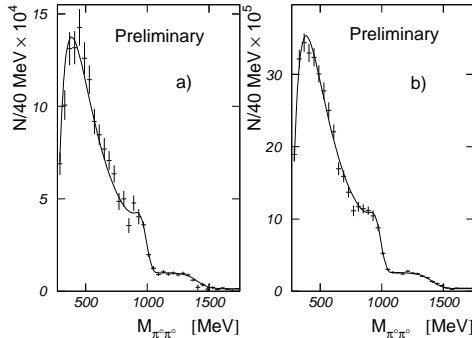


Figure 6: The  $|S|^2$  for the  $\pi^0\pi^0$  system produced in reaction (2) in the NA12/2 (a) and WA102 (b) experiments. The curves show fit with the sums of two relativistic Breit-Wigner functions and backgrounds.

$S$  wave have approximately the same heights in the three  $dP_T$  intervals, whereas the bump below 1 GeV becomes much more prominent for small  $dP_T$ . The  $f_2(1270)$  peaks are clearly seen in the  $D_0$  and  $D_-$  waves for large  $dP_T$  and disappear for small  $dP_T$ .

Table 1.  
Resonance production as a function of  $dP_T$  expressed as a percentage of its total contribution.  $dP_T$  intervals are given in GeV/c.

	$dP_T < 0.35$	$0.35 < dP_T < 0.6$	$dP_T > 0.6$
$f_0(980)$	$34 \pm 7$	$42 \pm 7$	$24 \pm 5$
$f_0(1300)$	$30 \pm 9$	$38 \pm 8$	$32 \pm 7$
$f_0(1500)$	$32 \pm 8$	$42 \pm 7$	$26 \pm 7$
$f_2(1270)$	not seen	$24 \pm 5$	$76 \pm 4$

Relative contributions of the resonances observed in the centrally produced  $\pi^0\pi^0$  system for three  $dP_T$  intervals have been estimated from a simultaneous fit to the NA12/2 and WA102 data (see sect. 7). These contributions are presented in table 1. The  $f_0(1300)$  and  $f_0(1500)$  have a similar behaviour as a function of the  $dP_T$  not consistent with that observed for  $q\bar{q}$  states. It is interesting to note that the enigmatic  $f_0(980)$  also does not behave as a normal  $q\bar{q}$  state. In contrast, the  $f_2(1270)$  is suppressed for small  $dP_T$  and enhanced for large  $dP_T$  in agreement with the behaviour of the other  $q\bar{q}$  states.

## 7. FIT TO THE $S$ WAVE

In order to determine the parameters of the scalar resonances, a fit to the  $S$  wave has been performed. The following parametrisation is used:

$$A(M_{\pi\pi}) = G(M_{\pi\pi}) + \sum_{n=1}^{N_{res}} a_n e^{i\theta_n} B_n(M_{\pi\pi}), \quad (4)$$

$$G(M_{\pi\pi}) = (M_{\pi\pi} - 2m_\pi)^\alpha e^{-\beta M_{\pi\pi} - \gamma M_{\pi\pi}^2} \quad (5)$$

where  $a_n$  and  $\theta_n$  are the amplitude and the phase of the  $n$ -th resonance, respectively,  $\alpha$ ,  $\beta$  and  $\gamma$  are the real parameters,  $B(M_{\pi\pi})$  is the relativistic Breit-Wigner function. To describe the  $|S|^2$ , function (4) module squared has been convoluted with a Gaussian to account the experimental mass resolution.

First, a fit to the  $S$  wave for the  $\pi^0\pi^0$  system produced in reaction (1) at 38 and 100 GeV/c has been carried out using four resonances (fig. 2). Three of them,  $f_0(980)$ ,  $f_0(1500)$  and  $f_0(2000)$ , correspond to the dips at 1, 1.5 and 2 GeV. One more resonance,  $f_0(1300)$ , is needed to describe the bump around 1.2 GeV. Without this resonance, quality of the fit deteriorates significantly. As a result of the  $f_0(1300)$  and  $f_0(1500)$  interference with the  $S$  wave background, the mass of the  $f_0(1300)$  turns out to be shifted to higher values as compared to the bump maximum, the  $f_0(1500)$  mass is also shifted as compared to the dip position. Parameters of the scalar resonances determined from the fit are presented in table 2.

Second, a fit to the reaction (2)  $S$  wave has been performed (fig. 6). To begin, two resonances are included in the fit to describe the shoulders at 1 and 1.4 GeV. A mass  $988 \pm 10$  MeV and a width  $76 \pm 20$  MeV of the first resonance are consistent with the tabulated parameters of the  $f_0(980)$  [10]. For the second resonance a mass of  $1420 \pm 30$  MeV and a width of  $230 \pm 50$  MeV are obtained. This state can be reproduced as a result of the  $f_0(1300)$  and  $f_0(1500)$  interference. The amount of the  $f_0(1300)$  is found to be about 20% of that of the  $f_0(1500)$ .

Finally, a simultaneous fit to the reaction (1) and (2)  $S$  wave has been performed. The  $f_0(980)$ ,  $f_0(1300)$ ,  $f_0(1500)$  and  $f_0(2000)$  are introduced to describe the  $S$  wave in reaction (1), only first three resonances are used in the fit to the  $S$  wave in reaction (2). Fit gives the  $f_0(980)$  and  $f_0(1300)$

masses consistent with those obtained from the fit to the charge exchange data, whereas a mass of the  $f_0(1500)$  is shifted to lower values. The  $f_0(1500)$  mass found from the simultaneous fit agrees well with the tabulated value [10], while the width turns out to be somewhat larger. As a result of the  $f_0(1500)$  mass shift, a mass of the  $f_0(2000)$  also becomes slightly smaller but agrees within the errors with the value obtained from the reaction (1)  $S$  wave fit. The state with a similar mass and width was observed by the WA102 Collaboration in the reaction  $pp \rightarrow p_f(\pi^+\pi^-\pi^+\pi^-)p_s$  [15].

Table 2.

Parameters (in MeV) of the scalar resonances obtained from the fit to the reaction (1)  $S$  wave (fit I) and the simultaneous fit to the reactions (1) and (2)  $S$  wave (fit II).

	Fit I		Fit II	
	Mass	Width	Mass	Width
$f_0(980)$	$970 \pm 10$	$85 \pm 20$	$980 \pm 10$	$80 \pm 20$
$f_0(1300)$	$1310 \pm 25$	$195 \pm 40$	$1300 \pm 25$	$220 \pm 40$
$f_0(1500)$	$1590 \pm 80$	$300 \pm 90$	$1495 \pm 35$	$250 \pm 60$
$f_0(2000)$	$2020 \pm 60$	$220 \pm 80$	$1960 \pm 60$	$210 \pm 80$

## 8. CONCLUSIONS

The partial wave analyses of the  $\pi^0\pi^0$  system produced in charge exchange  $\pi^-p$  reaction at 38 and 100 GeV/c and in central  $pp$  collisions at 450 GeV/c have been carried out. The  $f_0(980)$  and  $f_0(1500)$  appear in different ways in the two processes. These resonances are observed as dips in the  $S$  wave at 1 and 1.5 GeV in charge exchange reaction, whereas in central production the  $f_0(980)$  and  $f_0(1500)$  are seen as shoulders. The  $f_0(1300)$  is essential for the description of charge exchange data while in central production contribution of this resonance is less prominent. The centrally produced  $f_0(980)$ ,  $f_0(1300)$  and  $f_0(1500)$  have a similar dependence as a function of the  $dP_T$ , differed from that observed for all the undisputed  $q\bar{q}$  mesons.

An extra  $f_0(2000)$  state is observed in charge exchange reaction. It is similar to the scalar resonance observed by the WA102 Collaboration in the reaction  $pp \rightarrow p_f(\pi^+\pi^-\pi^+\pi^-)p_s$ . Existence of a new scalar state around 2 GeV may be very

important for understanding of the scalar nonet structure and for isolating the lightest scalar glueball.

For mesons with higher spins, production mechanisms of the  $f_2(1270)$ ,  $f_4(2050)$  and  $f_6(2510)$  as a function of momentum transfer in reaction (1) have been studied. All the three mesons are produced via a dominating one-pion exchange for small  $-t$ , whereas for large  $-t$  the  $f_2(1270)$  and  $f_4(2050)$  are produced predominantly through a natural-parity  $t$ -channel exchange. The  $f_2(1270)$  is clearly seen in the reaction (2)  $D_0$  and  $D_-$  waves for large  $dP_T$ . Its behaviour as a function of the  $dP_T$  is consistent with that expected for  $q\bar{q}$  state.

## REFERENCES

1. G.Bali *et al.*, Phys. Lett. **B309** (1993) 378.
2. J.Sexton *et al.*, Phys. Rev. Lett. **75** (1995) 4563.
3. V.V.Anisovich *et al.*, Phys. Lett. **B389** (1996) 388.
4. D.Alde *et al.*, Zeit. Phys. C **66** (1995) 375.
5. D.Alde *et al.*, Preprint IHEP 98-23, Protvino, 1998, submitted to Europ. Phys. Journal A.
6. F.Antinori *et al.*, Nuovo Cimento **A107** (1994) 1857.
7. S.U.Chung, Phys. Rev. **D56** (1997) 7299.
8. Yu.D.Prokoshkin, A.A.Kondashov and S.A.Sadovsky, Phys. Doklady **353** (1997) 323.
9. Yu.D.Prokoshkin and A.A.Kondashov, Phys. Doklady **336** (1994) 613.
10. Particle Data Group, Phys. Rev. **D52** (1996) 1.
11. V.V.Anisovich *et al.*, Phys. Lett. **B355** (1995) 363.
12. A.Kirk, hep-ex/9803024, submitted to Yadernaya Fizika.
13. D.Barberis *et al.*, Phys. Lett. **B397** (1997) 339.
14. F.E.Close and A.Kirk, Phys. Lett. **B397** (1997) 333.
15. D.Barberis *et al.*, Phys. Lett. **B413** (1997) 217.